JOURNAL OF MATERIALS SCIENCE **38** (2003) 909–915

Environmentally friendly polymer hybrids

Part I *Mechanical, thermal, and barrier properties of thermoplastic starch/clay nanocomposites*

HWAN-MAN PARK
Department of Polymer Science and Engineering, Pusan National University, Pusan 609-735, Korea

WON-KI LEE, CHAN-YOUNG PARK
Department of Polymer Science and Engineering, Pukyung National University, Pusan 608-739, Korea

WON-JEI CHO, CHANG-SIK HA*
Department of Polymer Science and Engineering, Pusan National University, Pusan 609-735, Korea
E-mail: csha@pusan.ac.kr

As an attempt to develop environmentally friendly polymer hybrids, biodegradable thermoplastic starch (TPS)/clay nanocomposites were prepared through melt intercalation method. Natural montrorillonite (Na^+ MMT; Cloisite Na^+) and one organically modified MMT with methyl tallow bis-2-hydroxyethyl ammonium cations located in the silicate gallery (Cloisite 30B) were chosen in the nanocomposite preparation. TPS was prepared from natural potato starch by gelatinizing and plasticizing it with water and glycerol. The dispersion of the silicate layers in the TPS hybrids was characterized by using wide angle X-ray diffraction (WAXD) and transmission electron microscopy (TEM). It was observed that the TPS/Cloisite Na^+ nanocomposites showed higher tensile strength and thermal stability, better barrier properties to water vapor than the TPS/Cloisite 30B nanocomposites as well as the pristine TPS, due to the formation of the intercalated nanostructure. The effect of clay contents on the tensile, dynamic mechanical, and thermal properties as well as the barrier properties of the nanocomposites were investigated.

1. Introduction

In recent years there has been a growing interest in the use of biodegradable polymers for packaging materials in order to reduce the environmental pollution caused by plastic wastes [1–3]. Starch is known to be completely biodegradable in soil and water and to be one of the most effective packing materials because it is a cheaply resourced material and has very fast biodegradability [4]. Starch promotes the biodegradability of a non-biodegradable plastic and also starch can be used together with a fully biodegradable synthetic plastic [5–8] producing biodegradable blends of low cost. The starch remains in granular form in the plastic matrix and thus may act as filler.

One major problem with granular starch composites is their limited processability, due to the big particle sizes (5–100 μm). Therefore, it is difficult to make blown thin film for package applications. For this reason, thermoplastic starch (TPS) has been developed by gelatinizing starch with 6–10% moisture with heat and pressure [9, 10]. Poor water resistance and low strength are limiting factors, however, for the use of materials manufactured only from TPS, and hence it is often blended with other polymers. For instance, it was found that the ductility of the gelatinized starch plasticized with approximately 15 wt% glycerol and 10 wt% water was improved by adding poly (ethylene-co-vinyl alcohol) (44 mol% ethylene) (EVOH) [11]. If the mechanical properties of the TPS can be further improved by the addition of a small quantity of an environmentally benign material, that polymer will find applications in more special or severe circumstances.

Organic-inorganic nanocomposites have attracted great interest since they exhibit unexpected hybrid properties synergistically derived from the two components [4, 12–16]. Melt intercalating polymers into the layered silicates of clay has been proven to be an excellent technique to prepare polymer-layered silicate (PLS) nanocomposites [16–23]. With only a few percent of clay, PLS nanocomposites exhibit greatly improved mechanical, thermal and barrier properties compared with the pristine polymers [24]. The essential

*Author to whom all correspondence should be addressed.

raw material for a nanoclay is montmorillonite (MMT), 2-to-1 layered-smectite clay with platy structure [16, 17]. Montmorillonite clays have been traditionally modified through a cationic ion substitution reaction with surface sodium ions [18, 19]. Applications of nanocomposites include packaging, automotive components, appliances, and so on.

More importantly, clay is environmentally friendly, naturally abundant and economic. To realize the combination of the biodegradability of cheap TPS and the high strength and stability of the clay, TPS/clay nanocomposites were prepared through melt intercalation method in the present work. So far very limited works have been reported on the preparation of biodegradable and/or environmentally-friendly PLS nanocomposites or hybrids [25–29]. In this sense, environmentally-friendly polymer blends and hybrids have been an important issue in this laboratory [29–31].

The objective of our research is to prepare the environmentally friendly nanocomposites from biodegradable TPS and clay, and to investigate the influence of the clay contents on the nanostructure and properties of the TPS/clay nanocomposites. The hybrids were characterized by Wide-angle X-ray diffraction (WAXD) and transmission electron microscopy (TEM). Tensile, dynamic mechanical, thermal and barrier property of the hybrids were measured.

2. Experimental

2.1. Materials

Cloisite 30B as an organically modified MMT and natural Na^+-MMT (Cloisite Na^+) were purchased from Southern Clay Co. The organoclay possesses methyl tallow bis-2-hydroxyethyl ammonium cations. Table I shows the related structure information and the X-ray diffraction peak positions of the clays used in this work.

The TPS was prepared using potato starch (PS: Katayama Co.), glycerol (95%, Junsei Chemical Co., Ltd), and water in the Haake Rheocord 600 system equipped with a mixer. The TPS was prepared using a two-step procedure; the premixture containing native potato starch/water/glycerol (5/2/3 by wt. ratio) was retained 1 hour to let plasticizers (water and glycerol) to swell the granular starch molecules. These swelled mixtures were transferred to the Haake mixer and the starch was gelatinized at 110°C for 25 minutes at 100 rpm of roller speed. The temperature and torque were monitored during the processing. After processing, the TPS samples were cooled and cut into small particles, in order to be premixed with clay powders easily.

TABLE I Structure information of organic clay of Cloisite Na^+ and Cloisite 30B

Organic clay[a]	Ammonium cation	XRD peak position (2θ)	Basal spacing (001)
Cloisite Na^+	None	7.85°	1.17 nm
Cloisite 30B	(CH_3) (T)$(CH_2CH_2OH)_2N^+$	4.73°	1.88 nm

T = tallow (~65%C18, ~30%C16, ~5%C14), anion:chloride.
[a]The surface hydrophobicity of Cloisite clays: 30B > Na^+.

2.2. Preparation of TPS/clay nanocomposites

TPS was melt intercalated with Cloisite clays in a Haake Rheocoder 600 roller mixer. First Cloisite Na^+ or 30B was dried under vacuum at 80°C for at least 24 hrs. Dried TPS and either of the two kinds of clays were mixed in the mixer at 110°C, 50 rpm for 20 minutes. The hybrids were then injection molded using a Mini-MAX molder (Custom Scientific Instruments, Inc., CS-183 MMX) to get dog-bone shaped specimens for characterization and property measurements. The blends after preparation were placed in tightly sealed polyethylene bags to prevent any moisture absorption.

2.3. Characterization

Wide Angle X-ray diffraction (WAXD) was performed using a Rigaku D/max 2200H X-ray diffractometer (40 kV, 50 mA) at a scanning rate of 0.5°/min. The basal spacing of the silicate layer, d, was calculated using the Bragg's equation, $\lambda = 2d \sin\theta$ (λ (Cu $K_{\alpha 1}$) = 0.15406 nm). TEM images were taken from cryogenically microtomed ultra thin sections using a Hitachi H-800 TEM.

2.4. Measurements

Tensile properties were measured using a Universal Testing Machine (Hounsfield UL25) at room temperature. The crosshead speed was 10 mm/min. All measurements were performed for five replicates of dog-bone shaped specimens and averaged to get the final result.

The apparatus and methodology described in the ASTM E96-80 were used to measure the water vapor transmission rate (WVTR) of the films [24]. Four films, 17 mm diameter discs, were prepared with 110 μm thickness and tested at 24 ± 2°C. Each specimen was sealed by a rubber O-ring on Plexiglas cups containing 60×10^{-6} m^3 saturated magnesium nitrate solution (54% relative humidity (RH)). There was an air gap of 17.95 mm between the solution and the underside of the specimen, and the test cups were placed in an air-tight plastic desiccators containing $CaSO_4$ desiccant (0% RH). The cups were 17.0 mm (inner diameter), 23.0 mm (outer diameter) and 76.5 mm (depth) with an exposed film area of 226 mm^2. The cups were weighed to the nearest 0.1 mg at 4 hour intervals during 24 hours. Regression analysis of weight loss as a function of time was performed to insure that accurate steady state slopes were obtained. WVTR was calculated by dividing the slope by the exposed film area.

Dynamic mechanical analysis (DMA) was carried out with a Rheovibron DDV-25F instrument (Orientec Co.) in the tension mode with the following parameters: frequency = 1 Hz; scan rate = 4°C/min; temperature range = −150°C to 130°C. Samples were prepared by injection molding using the Mini-Max moulder

and dried at 100°C in the chamber for 15 min to remove any residual bulk water before the measurements. The dynamic storage modulus (E'), loss modulus (E''), and mechanical loss tangent ($\tan\delta = E''/E'$) were measured.

Thermogravimetric analysis (TGA) was performed using a Perkin Elmer TGA 7 at a heating rate of 10°C/min under an atmosphere of flowing nitrogen (40×10^{-6} m^3/min). Samples (10–20 mg) were measured from room temperature to 500°C.

3. Results and discussion

3.1. Characterization of the TPS/clay nanocomposites

Fig. 1 shows the WAXD patterns of the TPS/Cloisite Na^+ nanocomposites with different clay contents as well as the pristine TPS and the Cloisite Na^+. The pristine TPS exhibited an amorphous X-ray diffraction pattern over the Bragg angles of 5–12°, as reported in the literature [28, 32]. The peak around 7.85° of the Cloisite Na^+ has shifted to around 4.5–5.0° for the TPS/Cloisite Na^+ nanocomposites regardless of the clay content, indicating the intercalated hybrid structures. The effect

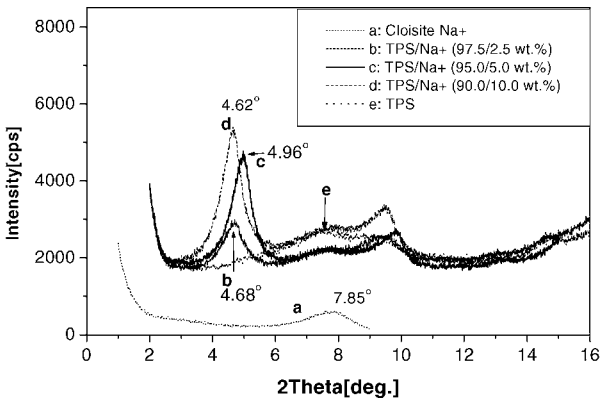

Figure 1 Effect of Cloisite Na^+ contents on the XRD patterns of TPS/Cloisite Na^+ nanocomposites.

of the clay content on the peak shift was not significant, even though the TPS/Cloisite Na^+ nanocomposite with 10 wt% of Cloisite Na^+ seems to exhibit the largest gap between the silicate layers.

In Fig. 2, the WAXD patterns of the TPS/Cloisite 30B nanocomposites with different clay contents are shown along with those of the pristine TPS and the Cloisite 30B. In comparison to the TPS/Cloisite Na^+ nanocomposites, the peak of the Cloisite 30B was shifted only slightly for the TPS/Cloisite 30B nanocomposites (from around 4.71° to around 4.30°). For the TPS/Cloisite 30B nanocomposite of 2.5 wt% Cloisite 30B content, however, no clear peak was observed around 4.30°, suggesting some exfoliation of small amounts of organoclays in the TPS matrix.

To further confirm the nanostructure of the TPS/clay hybrids and verify the conclusions from WAXD, TEM studies were carried out. Fig. 3 shows the TEM images of the hybrids with different clays and clay contents. The TEM images show that the TPS/Cloisite Na^+ hybrids show better dispersion and ordered intercalated structure than the TPS/Cloisite 30B hybrids and that the dispersion of clays becomes poorer on increasing the clay content. One can see big agglomerates of clay particles distributed in the TPS matrix for the TPS/Cloisite 30B with 10 wt% of clay content. If the clay content was over 10 wt%, the dispersion of clays in the TPS matrix became worse for both Cloisite Na^+ and Cloisite 30B hybrid systems, although data are not shown here.

In order for the polymer to fully wet and intercalate the clay or organoclay tactoids, it is imperative that the surface polarities of the polymer and clays or organoclays be matched [21]. Polar-type interactions are also critical for the formation of intercalated or exfoliated nanocomposites via polymer melt intercalation [33]. In most works dealing with PLS nanocomposites, organoclays show better dispersion in a polymer matrix than unmodified natural clays because of the general hydrophobicity of polymers. The TPS used in our work is, however, hydrophilic. Cloisite 30B possessing methyl

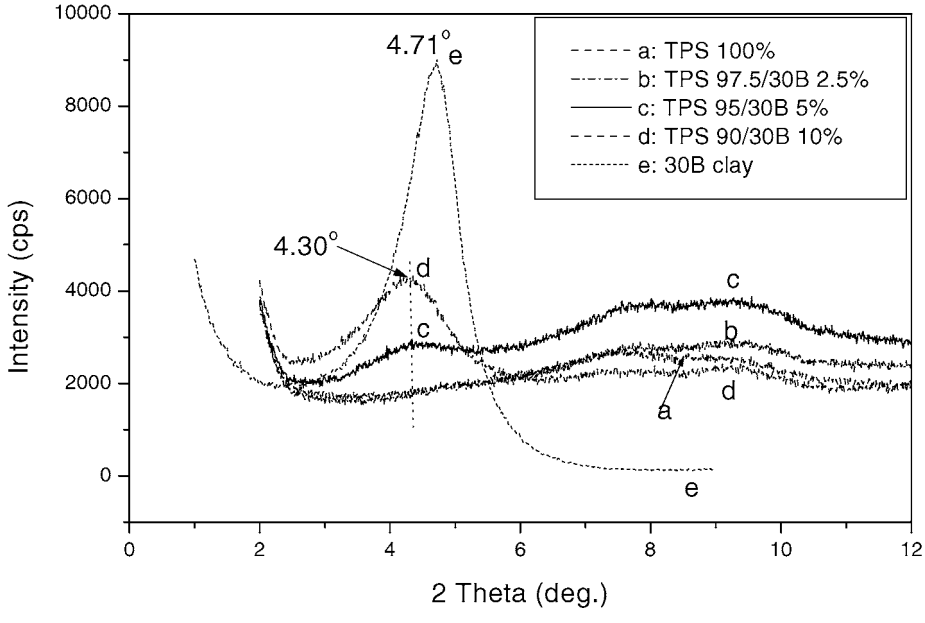

Figure 2 Effect of Cloisite 30B contents on the XRD patterns of TPS/Cloisite 30B nanocomposites.

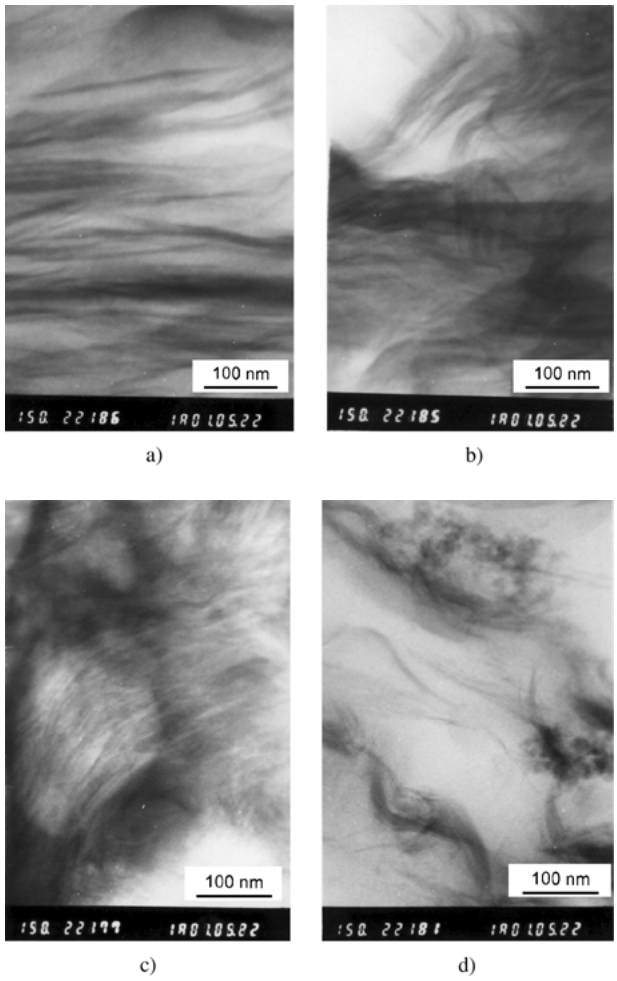

Figure 3 TEM images of various TPS/clay hybrids: (a) TPS95/Cloisite Na^+ 5 wt%, (b) TPS95/Cloisite Na^+ 10 wt%, (c) TPS95/Cloisite 30B 5 wt%, (d) TPS95/Cloisite 30B 10 wt%.

tallow bis-2-hydroxyethyl ammonium cations are much less hydrophilic than the natural Cloisite Na^+. Therefore, the Cloisite 30B does not match well with the polarity of TPS in comparison to the Cloisite Na^+. Furthermore, lack of strong polar interactions between the ammonium cations present in the Cloisite 30B and the TPS chains further discourages TPS intercalation. For these reasons, Cloisite 30B dispersed poorly, with large agglomerates present, and hardly formed a nanocomposite when introduced into the TPS matrix in comparison to the Cloisite Na^+.

It is expected, however, that the moderate surface polarity of Cloisite Na^+ is responsible for the formation of a partially intercalated TPS nanocomposite. In comparison to Cloisite 30B, therefore, the Na^+ cation gives Cloisite Na^+ the proper hydrophilicity and compatibility with TPS, which in turn favors intercalation. It is again seen that compatibility and optimum interactions between polymer matrix, organic modifiers and the silicate layer surface itself are crucial to the formation of intercalated as well as exfoliated PLS nanocomposite [34].

3.2. Tensile properties

Table II shows the tensile properties of the TPS/Cloisite Na^+ and the TPS/Cloisite 30B hybrids with different clay contents. It is seen that the tensile properties of the TPS/clay hybrids are generally increased with increasing clay content. It should be noted, however, that the TPS/Cloisite Na^+ nanocomposites showed higher tensile properties than the TPS/Cloisite 30B hybrids at the same contents, and that the TPS/Cloisite Na^+ nanocomposites with 5 wt% Cloisite Na^+ showed highest tensile properties among all the hybrids. The result is due to the stronger interaction between TPS and Cloisite Na^+ in comparison to that between TPS and Cloisite 30B, as discussed above. Comparison of Figs 1 through 3 and Table II indicates that the better dispersion of clays in the TPS matrix gives the stronger mechanical properties.

TABLE II Tensile properties of TPS/clay nanocomposites with various amounts of Cloisite Na^+ and Cloisite 30B

	Property	
Blend composition	Tensile strength (MPa)	Elongation at break (%)
TPS 97.5/Na^+ 2.5 wt%	2.79	48.9
TPS 95/Na^+ 5.0 wt%	3.32	57.2
TPS 90/Na^+ 10.0 wt%	3.20	52.0
TPS 97.5/30B 2.5 wt%	2.75	45.7
TPS 95/30B 5.0 wt%	2.80	44.5
TPS 90/30B 10.0 wt%	3.00	45.7
TPS 100 wt%	2.61	47.0

3.3. Water vapor transmission rate (WVTR)

Fig. 4 shows the relative water vapor transmission rate (WVTR) (hybrid WVTR/polymer WVTR, P_c/p_p) versus the contents of Cloisite Na^+ or Cloisite 30B in the TPS matrix. Fig. 4 shows that for the TPS hybrid films the WVTR decreased remarkably with adding small amounts of clays for both Cloisite Na^+ and 30B. It means that the layered structure of clay blocks the transmission of moisture vapor through the film matrix. It is interesting to note that in Fig. 4 the relative WVTR of the TPS nanocomposites was reduced by nearly a half compared to the pristine TPS at only 5 wt% of silicate. The dramatic lowering of WVTR in

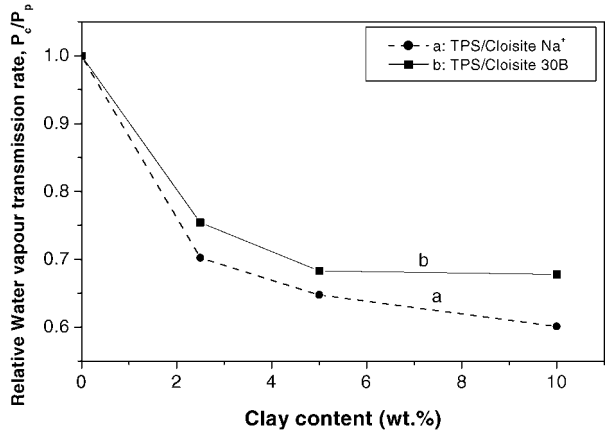

Figure 4 Effect of Cloisite Na^+ or Cloisite 30B contents on the relative water vapour transmission rate behavior of TPS/Cloisite Na^+ and 30B nanocomposites at 24°C.

the nanocomposites is due to the presence of dispersed large aspect ratio silicate layers in the polymer matrix as seen in other polymer-layered silicate composites [35, 36].

This forces water moisture traversing the film to follow a tortuous path through the polymer matrix surrounding the silicate particles, thereby increasing the effective path length for diffusion. Complete delaminating of the clay leads to the formation of high aspect ratio (100–1000) impermeable layers, which is expected to maximize barrier properties as predicted by Cussler *et al*. [37]. The observed dramatic decrease in WVTR is of great importance in evaluating TPS composites for use in food packaging, protective coatings, and other applications where efficient polymeric barriers are needed. For these applications, significant reduction in WVTR can result in either increased barrier efficiency, or reduced thickness of the barrier layer for the same efficiency. Furthermore, reduced WVTR in biodegradable polymer composite films may have the added benefit for modifying degradation rates, because hydrolysis of the matrix polymer is likely to depend on the transport of water from the surface into the bulk of the material [25]. Since the film rigidity is improved by the addition of clay, the amount of clay added to the composite film should be controlled due to its synergetic effects on the mechanical strength and WVTR of the film.

Fig. 4 also shows that the barrier property to water vapor is better for the TPS/Cloisite Na^+ nanocomposite than for the TPS/Cloisite 30B nanocomposite, regardless of the clay contents. Again, we note that the better dispersion of clays in the TPS matrix gives the better barrier properties.

3.4. Dynamic mechanical properties

Figs 5 and 6 show the temperature dependence of the relative storage modulus (E'_c/E'_p) and tan δ for the pristine TPS and the nanocomposites intercalated with 2.5–10 wt% of Cloisite Na^+, where E'_c and E'_p are the storage modulus of nanocomposites and the pristine polymer, respectively.

When 2.5 wt% of clay was added to TPS (Fig. 5b), no significant difference in E'_c/E'_p can be seen over

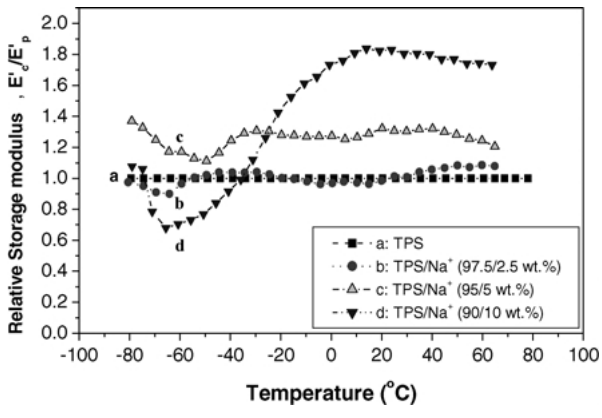

Figure 5 Effect of Cloisite Na^+ contents on the relative storage modulus behavior of TPS/Cloisite Na^+ nanocomposites.

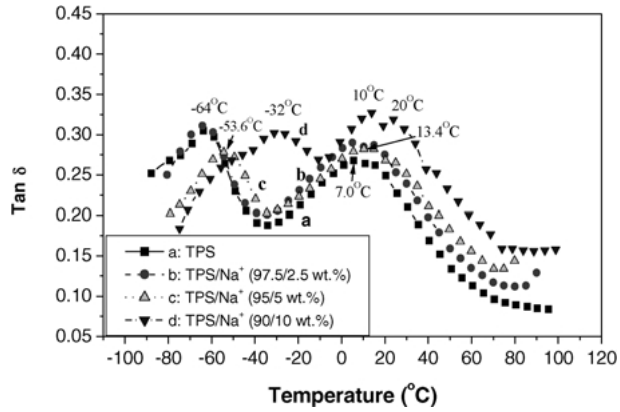

Figure 6 Effect of Cloisite Na^+ contents on the tan δ behavior of TPS/Cloisite Na^+ nanocomposites.

the investigated temperature ranges, indicating that intercalated nanocomposites do not strongly influence the elastic properties of the matrix. On the other hand, for both the hybrids containing 5 and 10 wt% Cloisite Na^+, the storage modulus increased by 20–50% with increasing clay contents compared to the pristine TPS in the temperature range -20°C to 80°C. It is important to note the enhanced storage modulus at temperatures above room temperature for intercalated nanocomposites filled with layered silicates of high aspect ratio, especially for the TPS/Cloisite Na^+ hybrid. A possible explanation for such an improvement could be the creation of a three-dimensional network of interconnected long silicate layers, strengthening the material through mechanical percolation [38, 39].

The smaller E'_c values in comparison to other hybrids and TPS at low temperature around -60 to -20°C, when the contents of Cloisite Na^+ is high (10 wt%), may be related to the increasing glass transition temperature in the presence of lots of clay, which affects the stiffness of the parent starch backbone of the TPS. The shift of tan δ peaks of the TPS/Cloisite Na^+ 10 wt% hybrid towards much higher temperatures (-64°C to -32°C, 7.0°C to 10–20°C, respectively) in Fig. 6 may prove the fact. The result may be attributed to several factors including interaction between starch granules and clay, etc. at the low temperature ranges. In Fig. 6, the two transition peaks around -64°C and 7.0°C of TPS are due to respectively the α-relaxation of starch and the β-relaxation of glycerol [40]. The temperatures at which the two transition peaks were observed were increased with increasing clay contents.

Figs 7 and 8 show the temperature dependence of the relative storage modulus (E'_c/E'_p) and tan δ for the pristine TPS and the nanocomposites intercalated with 2.5–10 wt% of Cloisite 30B. On increasing the clay contents, the storage modulus was increased but all the values were less than that of the pristine TPS over the almost entire temperature ranges investigated. It means that when the hybrid shows bad dispersion of clays in a polymer matrix, as already shown in Figs 2 and 3, the addition of small amounts of clays does not enhance the modulus of the TPS matrix. The tan δ behavior in Fig. 8 shows that the two transition temperatures are shifted to lower temperatures due to the

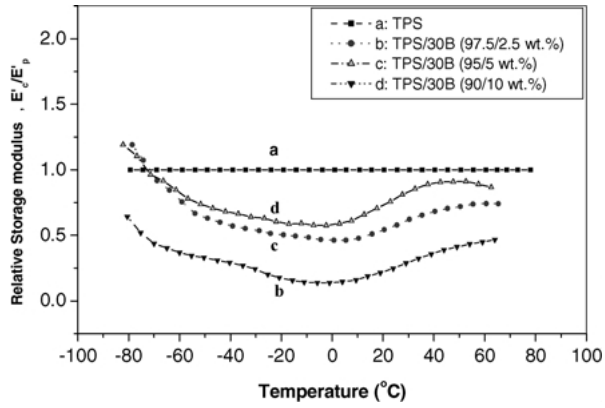

Figure 7 Effect of Cloisite 30B contents on the relative storage modulus behavior of TPS/Cloisite 30B nanocomposites.

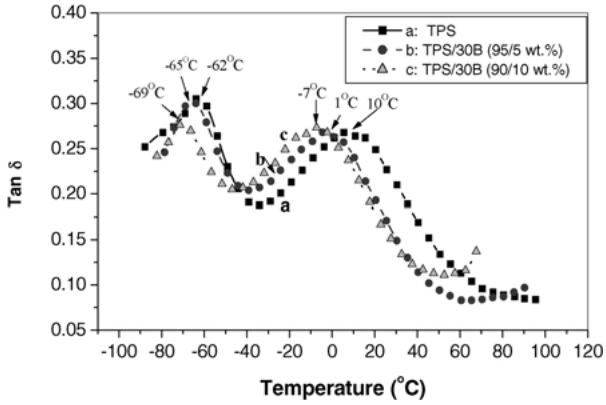

Figure 8 Effect of Cloisite 30B contents on the tan δ behavior of TPS/Cloisite 30B nanocomposites.

repulsion between hydrophilic TPS and the hydrophobic organoclays, which is in contrast to the case of the TPS/Cloisite Na^+ nanocomposites. The trend becomes more distinct as the clay contents are increased.

3.5. Thermal stability

The thermal stability of a material is usually assessed by thermogravimetric analysis (TGA) where the sample mass loss due to volatilization of degraded by-products is monitored as a function of a temperature ramp [22]. Figs 9 and 10 show respectively the TGA curves of

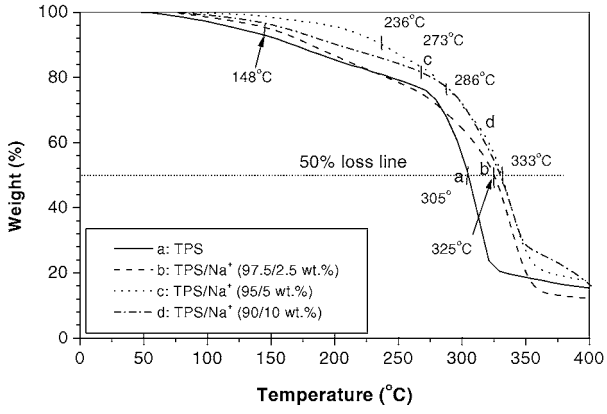

Figure 9 Effect of Cloisite Na^+ contents on the TGA curve of TPS/Cloisite Na^+ nanocomposites.

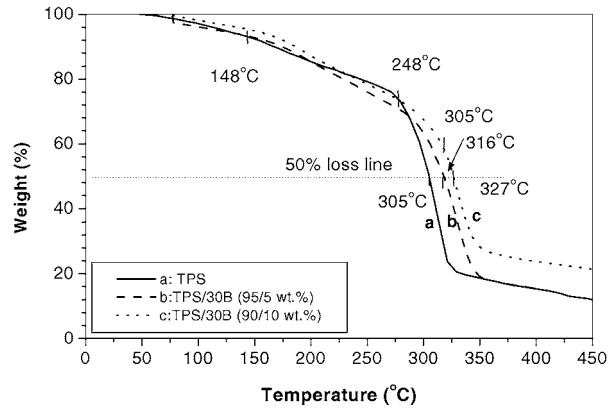

Figure 10 Effect of Cloisite 30B contents on the TGA curve of TPS/Cloisite 30B nanocomposites.

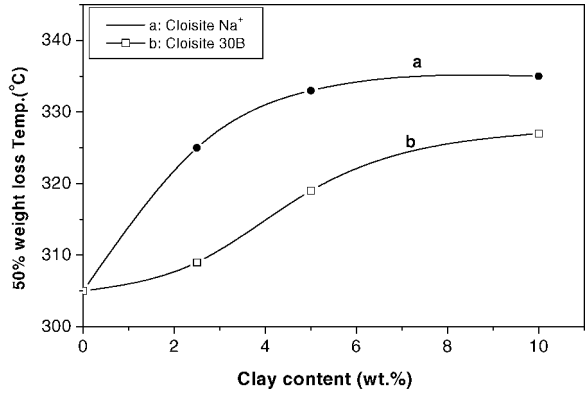

Figure 11 Effect of Cloisite Na^+ and 30B contents on the temperature at which 50% of weight is lost from TGA curve of TPS/Cloisite Na^+ or 30B nanocomposites.

TPS/Cloisite Na^+ and 30B hybrids. Based on the TGA curves of the two hybrids, the temperature at which 50 wt% weight loss takes place is shown in Fig. 11 for TPS/Cloisite Na^+ and TPS/30B hybrids. The temperature of 50% weight loss of the TPS/Cloisite Na^+ (95/5 w./w.) hybrid increased from 305°C to 336°C, meaning that the thermal stability was noticeably increased as compared to the pristine TPS. The increase of the thermal stability with the addition of clays up to 5 wt% was significant for both kinds of clays, while the increase was leveled off with further increasing clay content. It is seen that the thermal stability of TPS/Cloisite Na^+ and TPS/Cloisite 30B hybrids are better than that of the pristine TPS. Note also that the TPS/Cloisite Na^+ nanocomposites showed better thermal stability than TPS/Cloisite 30B hybrids do, regardless of the clay content. The results of Figs 9 through 11 strongly indicate that the enhancement of the thermal stability of the TPS with the addition of clays is larger when the TPS based hybrids form intercalated nanocomposites than when they do not, proving that the better dispersion of clays in the TPS matrix gives better thermal stability as well as mechanical properties.

4. Conclusions

Novel biodegradable thermoplastic starch (TPS)/clay nanocomposites were prepared through melt

intercalation method as an attempt to develop environmentally friendly polymer hybrids. Two different kinds of clays, Cloisite 30B with ammonium cations located in the silicate gallery and one unmodified Cloisite Na^+ montmorillonite (MMT), were chosen in the nanocomposite preparation. Cloisite Na^+ MMT showed better dispersion in the nanostructure of the TPS hybrids. The dispersion of the clays in the TPS matrix depends on the hydrophilicity of the clays and especially the polar interaction between the silicate layers and TPS. The strong interaction between TPS and Cloisite Na^+ leads to higher tensile properties and lower water vapor transmission rate than the pristine TPS. The results also showed that adding only 5 wt% of clays to the TPS matrix is favorable to improve the tensile strength and barrier property of these composites.

For both the hybrids of 5 and 10 wt% Cloisite Na^+, storage modulus increased by 20–50% with increasing clay content compared to the pristine TPS in the temperature range $-20°C$ to $80°C$. The tan δ data of the TPS/Cloisitie Na^+ nanocomposites showed that the two transition peaks around $-64°C$ and $7.0°C$ of TPS, which were due to the glass transition of starch and the glass transition of glycerol, respectively, were shifted towards higher temperatures on increasing clay content. The TGA curve showed that TPS/Cloisite Na^+ nanocomposites exhibit better thermal stability than the TPS/Cloisite 30B nanocomposites do at the same clay contents. It was concluded that the better the dispersion of the clays in the TPS matrix the better mechanical, thermal, and barrier properties when we compare the TPS/Cloisite Na^+ and the TPS/Cloisite 30B hybrids with different clay contents.

Acknowledgements

The work was supported by the Center for Integrated Molecular Systems, POSTECH, Korea and the Brain Korea 21 Project in 2001. The authors wish to express their sincere thanks to Prof. Xiucuo Li, Hebei University of Technology, P. R. China, for her help in TEM measurements. The work is dedicated to Prof. Jung Il Jin, Korea University, for his 60th birthday.

References

1. H. RAKEUCHI and C. COHEN, *Macromolecules* **32** (1999) 6792.
2. J. A. BRYDSON, in "Plastic Materials," 3rd ed. (Butterworth & Co, London, 1975) p. 1.
3. G. L. ROBERTSON, in "Food Packaging" (Marcel Dekker, New York, 1993).
4. A. OVA, Y. KUROKAWA and H. YASUDA, *J. Mater. Sci.* **35** (2000) 1045.
5. A. USUKI, T. MIZUTANI, Y. RUKUSHIMA, M. FUJIMOTO, K. FUKUMORI, Y. KOJIMA, N. SATO, T. KURAUCHI and O. KAMIGAITO, US Patent 4,889,885 (1989).
6. Y. YANG, Z. ZHU, J. YIN, X. WANG and Z. QI, *Polymer* **40** (1999) 4407.
7. L. BIASCI, M. AGLIETTO, G. RUGGERI and F. CIARDELLI, *ibid.* **35** (1994) 3296.
8. D. C. LEE and L. W. JANG, *J. Appl. Polym. Sci.* **61** (1996) 117.
9. E. R. GEORGE, T. M. SULLIVAN and E. H. PARK, *Polym. Eng. Sci.* **34** (1994) 17.
10. A. USUKI, Y. KOJIMA, M. KAWASUMI, A. OKADA, Y. FUKISHIMA, T. KURAUCHI and O. KAMICAITO, *J. Mater. Res.* **8** (1993) 1179.
11. C. D. MUZNY, B. D. BUTLER, H. J. M. HANLEY, F. TSVETKOV and D. G. PEIFFER, *Mater. Lett.* **28** (1996) 379.
12. M. KATO, A. USUKI and A. OKADA, *J. Appl. Ploym. Sci.* **66** (1997) 1781.
13. Y. FUKUSHIMA, A. OKADA, M. KAWASUMI, T. KURAUCHI and O. KAMIGAITO, *Clay Miner.* **23** (1988) 27.
14. R. GANGOPADHYAY and A. DE, *Chem. Mater.* **12** (2000) 608.
15. H. J. CHOI, S. G. KIM, Y. H. HYUN and M. S. JHON, *Macromol. Rapid. Comm.* **22** (2001) 320.
16. N. HASEBAWA, M. KAWASUMI, M. KATO, A. USUKI and A. OKADA, *J. Appl. Polym. Sci.* **67** (1998) 87 and references therein.
17. K. A. CARRADO, *Appl. Clay Sci.* **17** (2000) 1.
18. Special issue on "Nanostructured Materials," *Chem. Mater.* **8** (1996) 1569 and references therein.
19. R. KIRSHNAMOORTI, R. A. VAIA and E. P. GIANNELIS, *ibid.* **8** (1998) 1728.
20. A. USUKI, A. KOIWAI, Y. KOJIMA, M. KAWASUMI, A. OKADA, T. KURAUCHI and O. KAMIGAITO, *J. Appl. Polym. Sci.* **55** (1995) 119.
21. P. C. LEBARON, Z. WANG and T. J. PINNAVAIA, *Appl. Clay Sci.* **15** (1999) 11.
22. M. ALEXANDRE and P. DUOIS, *Mater. Sci. Eng.* **28** (2000)1.
23. M. ZANETTI, S. LOMAKIN and G. CAMINO, *Macromol. Mater. Eng.* **279** (2000) 1.
24. T. H. MCHUGH, R. A. BUSTILLOS and J. M. KROCHTA, *J. Food. Sci.* **58** (1993) 899.
25. P. B. MESSERSMITH and E. P. GIANNELIS, *J. Polym. Sci., Part A: Polym. Chem.* **33** (1995) 1047.
26. J. A. TETTO, D. M. STEEVES, E. A. WELSH and B. E. POWELL, *ANTEC* (1999) 1628.
27. S. T. LIM, Y. H. HYUN and H. J. CHOI, *Chem. Mater.* **14** (2002) 1839.
28. M. VIKMAN, S. H. D. HULLEMAN, M. VAN DER ZEE, P. MYLLARINEN and H. FEIL, *J. Appl. Polym. Sci.* **74** (1998) 2594.
29. W. K. LEE, Y. DOI and C. S. HA, *Macromol. Biosci.* **1** (2001) 114.
30. C. S. HA and W. J. CHO, *Prog. Polym. Sci.* **27** (2002) 759.
31. S. R. LEE, H. M. PARK, H. T. LIM, T. K. KANG, X. LI, W. J. CHO and C. S. HA, *Polymer* **43** (2002) 2495.
32. J. J. G. VAN SOEST, K. BENES and D. DE WIT, *ibid.* **37** (1996) 3543.
33. R. A. VAIA and E. P. GIANNELIS, *Macromolecules* **30** (1997) 8000.
34. X. LI, T. K. KANG, W. J. CHO, J. K. LEE and C. S. HA, *Macromol. Rapid. Comm.* 22 (2001) 1310.
35. Y. KOJIMA, K. KUKUMORI, A. USUKI, A. OKADA and T. KURAUCHI, *J. Mater. Sci. Lett.* **12** (1993) 889.
36. K. YANO, A. USUKI and A. OKADA, *J. Polym. Sci., Part A: Polym. Chem.* **35** (1997) 2289.
37. E. L. CUSSLER, S. E. HIGHES, W. J. WARD and R. ARIS, *J. Mem. Sci.* **38** (1998) 161.
38. W. J. WARD, G. L. GAINES, M. M. ALGER and T. J. STANLEY, *ibid.* **55** (1991) 173.
39. T. LAN, P. D. KAVIRATNA and T. J. PINNAVAIA, *Chem. Mater.* **6** (1994) 573.
40. L. AVEROUS, N. FAUCONNIER, L. MORO and C. FRINGANT, *J. Appl. Polym. Sci.* **76** (2000) 1117.

Received 23 May
and accepted 10 October 2002